

Experiment report

Phase contrast imaging using synchrotron mammography

P. Monnin, M. Pachoud, F.R. Verdun

Institut universitaire de radiophysique appliquée – Grand Pré 1 – CH 1007 Lausanne Suisse

Experiment reference : LS-2097

Beamline : BM05

Shifts : 12

Date of experiment : 29.01.2002 – 03.02.2002

Local contact : Dr. J. Hoszowska

1. Introduction

The aim of the experiments was to utilize the coherence properties of a third generation synchrotron source to produce phase contrast images using the in-line holographic technique. Images of very simple physical objects were recorded in several different conditions which allowed the observation of the phenomena due to the coherent properties of the wave front. The comparison of the recorded images with the predicted image formation from the theory of phase contrast will allow to reveal the performances of this technique in terms of sensitivity, geometrical requirements and energy level. Further images of a pork kidney have also been produced with various distances between the object and the screen-film system. After a 1 meter distance tremendous edge-enhanced effects appear and allow the detection of very fine low contrasted structures unnoticed with no or low phase contrast effects.

2. Materials and methods

Images were recorded on a mammographic x-ray film Kodak Min-R 2000 without screen. The images were obtained by scanning vertically the detector and the test objects with two step to step motors. The beam borders were “cleaned” with a tungsten slit placed at the output of the beam. The adjustment of the slit height allowed the choice of the dose rate and the optical density of the film in the range of the motor speeds available. Scattering effects on the images were controlled by placing a 1 mm wide copper slit between the object and the detector.

A set of cylindrical wires from 10 μm to 1 mm diameter and different materials (nylon, aluminum and copper) was first employed to study the physical behavior of the edge-enhancement effects at different object to film distances. Another set of sharp edges (step or Heaviside functions) of 200 μm thickness of PMMA, aluminum and Teflon, placed perpendicular to the beam, produced also phase contrast effects in a wide range of spatial frequency. The image produce will allow the description of the contrast transfer function (CTF) of the system for different object to film distances and energies. It will result in a better comprehension of the geometrical parameters and energy requirements to optimize the contrast enhancement effects when dealing with biological tissues. Several of these test objects were investigated in air and in a small box of PMMA filled with water to study the effect of relative electronic densities differences on the edge enhancement effects.

All images were digitalized on a Tango Heidelberg digitalizer with a resolution of 4 μm and an aperture diameter of 15.9 μm .

3. Experimental results

a) wires

The phase contrast image of a wire can be simulated by means of the Fresnel-Kirchhoff integral. The effect of a cylindrical wire on a spherical monochromatic wave E_0 is given by the following equation :

$$E(x, y, z) = E_0(x, y, z) \sqrt{\frac{z}{i\lambda R_0 R}} \exp\left\{ik \frac{(x - x_s)^2}{2z}\right\} \int_{-r}^r \exp\left\{ik \left[\frac{(\chi - x_s)^2}{2R_0} + \frac{(x - \chi)^2}{2R} \right]\right\} F(\xi) d\xi$$

where : k is the wave number

λ is the wavelength of the radiation

R is the object to detector distance

R_0 is the source to object distance

$z = R + R_0$ is in the direction of the propagation of the x-rays

(x_s, y_s) are the coordinates of the point source

(x, y) are the lateral coordinates in the plane on the detector

(x, h) are the lateral coordinates in the plane on the object

r is the radius of the wire

E_0 is the spatial part of the incident spherical monochromatic wave propagating along the z direction :

$$E_0(x, y, z) = \frac{1}{z} \exp\left\{ik \left[z + \frac{(\xi - x_s)^2 + (\eta - y_s)^2}{2z} \right]\right\}$$

The transmission function of a homogeneous cylindrical object is given by :

$$F(\xi) = \exp\left\{-\frac{4\pi}{\lambda} (\beta + i\delta) \sqrt{r^2 - \xi^2}\right\}$$

where b and d are respectively the real and imaginary parts of the complex refractive index

The image is calculated in the (x, y) detector plane as the intensity normalized to the background intensity :

$$I(x, y) = |E(x, y) E^*(x, y)| \quad , \quad \text{where } E^* \text{ is the complex conjugate of the electric field } E$$

To reduce the noise on the measurements, 100 adjacent profiles were averaged. The resulting profile was converted into relative exposure and relative intensity by means of the sensitometric curve of the film. Figures 1 to 4 show that numerical simulations of the wire images for the different conditions announced in the previous paragraph are in good

agreement with the experimental results. The solution of the Fresnel-Kirchhoff was filtered considering a $10\ \mu\text{m}$ resolution in order to take into account the limited resolution of the image detector. Images were obtained without screen in front of the film.

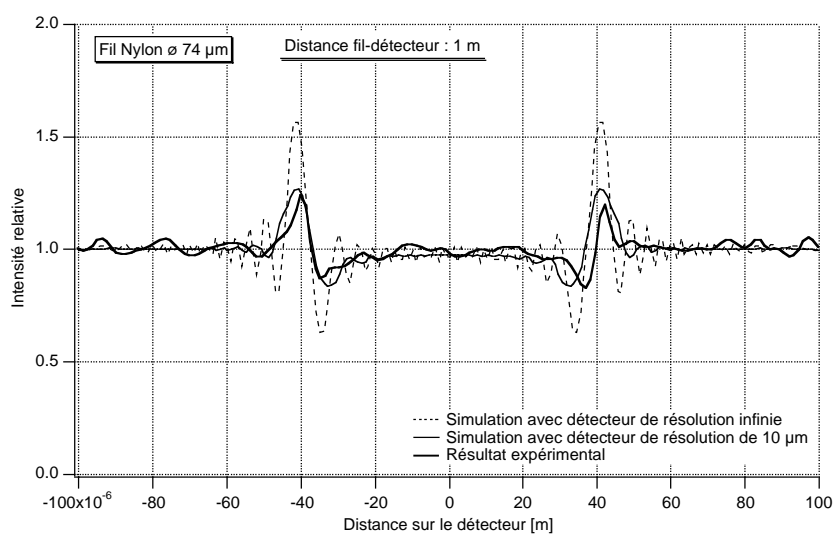


Figure 1 : Comparison between the simulated and the experimental image of a $74\ \mu\text{m}$ in diameter nylon's wire with a distance object to detector of 1 m.

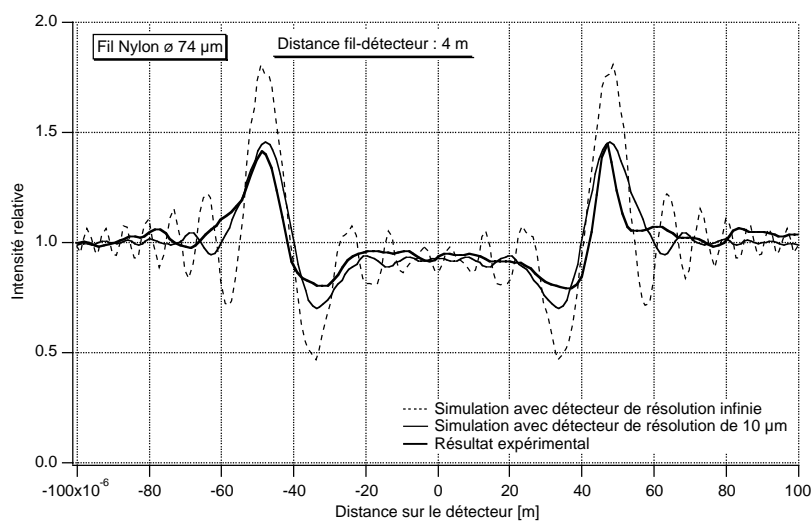


Figure 2 : Comparison between the simulated and the experimental images of a $74\ \mu\text{m}$ in diameter nylon's wire with a distance object to detector of 4 m, where phase contrast effect is increased.

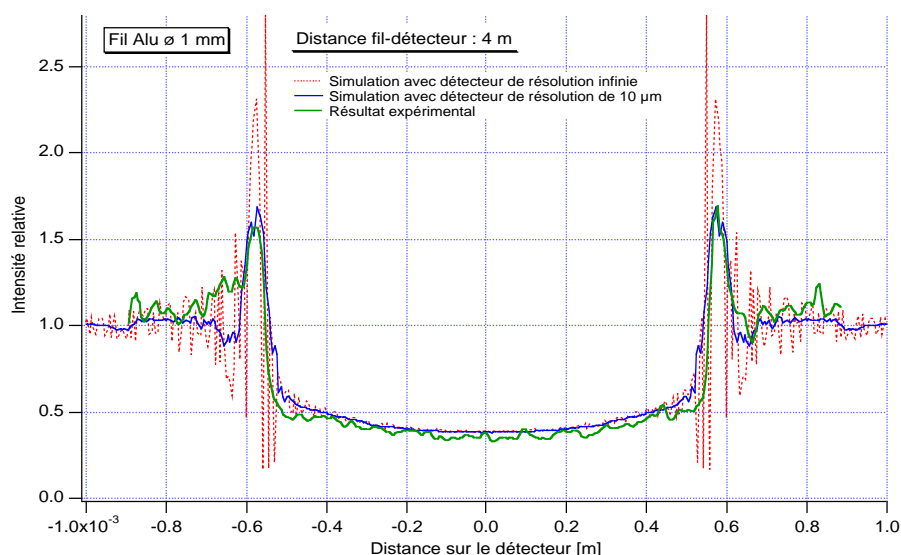


Figure 3 : Comparison between the simulated and the experimental images of a 1 mm in diameter aluminum wire with a distance object to detector of 4 m. The X-ray absorption contrast is superimposed to the phase contrast.

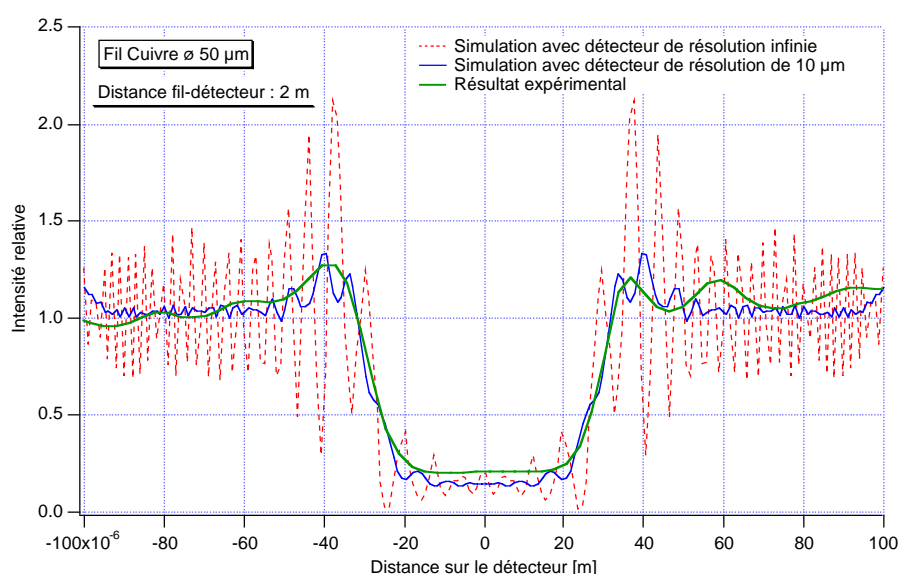


Figure 4 : Comparison between the simulated and the experimental images of a 50 μm in diameter copper wire with a distance object to detector of 2 m. The phase contrast is not as pronounced as for the nylon wires.

b) sharp edges

The sharp edge data are now under study. The edge spread function (ESF) from the sharp edges will be estimated by measuring the profiles along 256 pixels in gray level units. To reduce noise on measurements, 100 adjacent profiles will be averaged. As in the previous experiment, the ESF will be converted into relative exposure and intensity using the sensitometric curve of the film. The line spread function (LSF) will be calculated by differentiating the ESF. The contrast transfer function (CTF) will be obtained from the LSF by Fourier transform. The CTF will be measured for several materials at different distances. It will provide the geometrical and physical conditions that maximize the phase contrast effects versus the spatial frequency of the imaged object.

c) images of a pork kidney

In order to demonstrate the potential of phase-contrast effects on biological tissue samples, phase and absorption contrast images of a pork kidney were recorded at 20 keV using different object to film distances (figures 4 and 5), with a screen-film system. They demonstrate the considerable potential of the edge-enhanced effects to improve the image contrast of biological tissues. The effects of phase modulations reveal an important improvement of small structures visibility due to edge enhancement. It shall be pointed out that all these images have been obtained with the same dose.

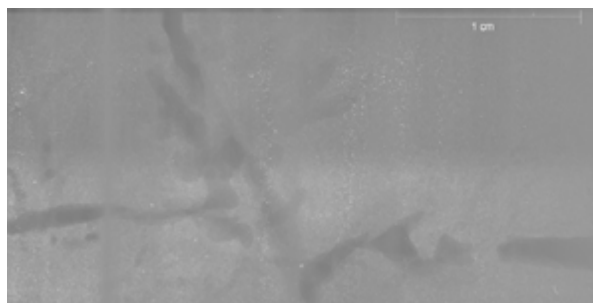


Figure 4 : Part of a pork kidney imaged at 20 keV with an object to film distance of 0.2 m

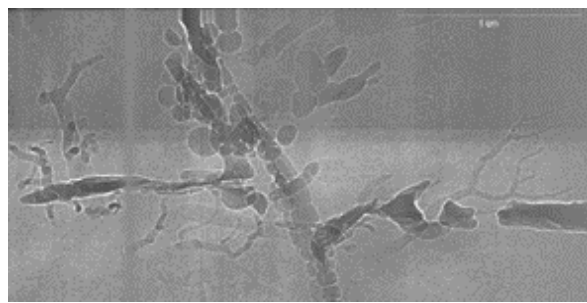


Figure 5 : Part of a pork kidney imaged at 20 keV with an object to film distance of 4 m

5. Conclusion

Images of simple wires in different conditions allow the reconstruction of the weak perturbations of the coherent incident wave front and permit to reveal the performances of these techniques in terms of sensitivity to geometrical requirements and energy levels. The experimental results are in good agreement with the theory predictions. Phase contrast images of sharp edges will permit the calculation of the CTF for several materials and different object to detector distances. It will provide the sensitivity of phase contrast effects versus the spatial frequency of the imaged object. Further images of biological tissues reveal the potential of in-line holography technique on biological tissue samples and show the considerable potential of the edge-enhanced effects to improve the image contrast. One application we wish to pursue is the imaging of micro-vascularization where X-ray absorption contrast is also absent. The first objective we had was to find an application in the field of mammography, in particular in improving the pathology classification of breast lesion. However, pathology classification relies more on cells anti-genetic properties than of macroscopic structures. Micro-vascularization study is a certainly more promising area.

The preliminary results reported here show that the shifts corresponding to the LS-2097 were very successful. More time is now required to analyze all the films produced. The next milestone is now to publish our results.